JACS Au
AN OPEN ACCESS JOURNAL OF THE AMERICAN CHEMICAL SOCIETY

pubs.acs.org/jacsau
Article

Stabilizing Highly Reactive Aryl Carbanions in Water Microdroplets: Electrophilic *Ipso*-Substitution at the Air–Water Interface

Abhijit Nandy, Hariharan T, Deepsikha Kalita, Debasish Koner, and Shibdas Banerjee*

Cite This: *JACS Au* 2024, 4, 4488–4495
Read Online
ACCESS | Metrics & More | Article Recommendations | Supporting Information

ABSTRACT: The fleeting existence of aryl carbanion intermediates in the bulk phase prevents their direct observation and spectroscopic measurement. In sharp contrast, we report the direct interception of such unstable species at the air–water interface of microdroplets. We observed the transformation of three types of aryl acids (benzoic, phenylsulfinic, and phenylboronic acids) into phenyl carbanion (Ph^-) in water microdroplets, as examined by mass spectrometry. Experimental and theoretical evidence suggests that the high intrinsic electric field at the microdroplet surface is likely responsible for cleaving the respective acid functional groups of these substrates, generating Ph^-, which can subsequently be trapped by an electrophile, including a proton, to yield the corresponding *ipso*-substitution product. While catalyst-free decarboxylation at ambient temperature is challenging in the bulk phase, we report over 30% instantaneous conversion of benzoic acid to Ph^- in sprayed aqueous microdroplets in less than a millisecond. Thus, this study lays the foundation of a green chemical pathway for the aromatic electrophilic *ipso*-substitution reaction by spraying an aqueous solution of aryl acids, eliminating the need for any catalyst or reagent.

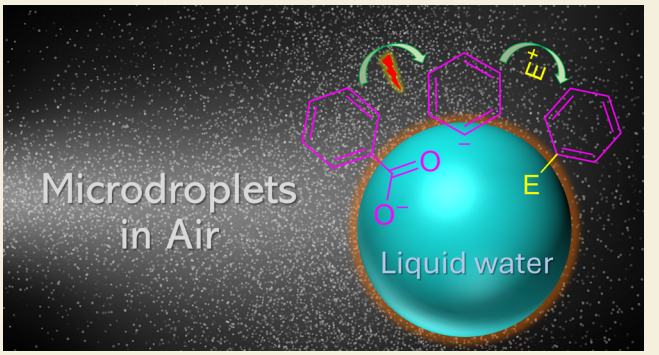

KEYWORDS: *microdroplet surface, interfacial electric field, aryl acids, aryl carbanions, ipso-substitution, mass spectrometry*

INTRODUCTION

Water acts as an inert solvent in the bulk for many chemical substances but transforms into a powerful reactor when it forms microdroplets. Recent discoveries of several unusual chemical properties and reactions at the air–water interface have hinted at the potential future of water microdroplet chemistry in sustainable developments.[1−16] The air–water interface of microdroplets is a chaotic boundary with highly anisotropic structural features of water, leading to unique characteristics such as a high intrinsic electric field (>10^7 V/cm) on the surface[17,18] and the prevalence of reactive oxygen species.[19−24] Since such a high electric field exceeds the dielectric strength of air (0.03 MV/cm), electrical breakdown of air becomes feasible at the air–water interface, which we recently verified experimentally.[25] It has been observed that the thermodynamics of chemical processes is altered in microdroplets, enabling the progression of thermodynamically unfavorable reactions under ambient temperature at the air–water interface.[26−33] Recently, our group has demonstrated the spontaneous generation and stabilization of aryl carbocations from phenols in aqueous microdroplets, allowing them to be converted into value-added chemicals through the nucleophilic attack at the air–water interface, which is otherwise challenging to achieve in the analogous bulk phase.[1] This finding motivated us to search for chemical precursors capable of decomposing at the air–water interface of microdroplets to produce aryl carbanions, another highly reactive species of fundamental significance in organic chemistry that has also barely been studied and utilized in the interfacial regime. Moreover, having access to such reactive species in useful amounts within an environmentally benign solvent (water) droplet should promote the establishment of green routes for synthesizing various aryl derivatives, with practical implications. Indeed, some of our recent studies suggested that water microdroplets can be harnessed to capture and stabilize various highly reactive alkyl carbocation and carbanion intermediates at the microdroplet surface.[34−38]

Thus, the present study introduces three classes of organic acids, namely, benzoic acid, phenylsulfinic acid, and phenylboronic acid, which undergo the loss of the respective acid functional groups at the water microdroplet surface, leading to spontaneous generation of highly reactive aryl carbanions without the need of any other catalyst or reagent. This has

Received: September 3, 2024
Revised: October 3, 2024
Accepted: October 7, 2024
Published: October 22, 2024

enabled us to achieve catalyst-free electrophilic *ipso*-substitutions of those aryl acids at the air−water interface. Decarboxylation, deboronation, and desulfination processes in aromatic systems typically require expensive transition metal and photoredox catalysts in bulk to facilitate the rupture of Csp^2−COOH, Csp^2−$B(OH)_2$, and Csp^2−SO_2H bonds.[39−42] Our experimental and theoretical investigations have revealed that the involvement of a high electric field and molecular orientation at the microdroplet surface enables such unusual chemistry to be attainable without a catalyst.

METHODS

Details of solvents, chemicals, gases, and computational methods are presented in the Supporting Information.

ESI-MS Study

A customized electrospray ionization (ESI) spray source coupled to an Orbitrap Exploris 120 mass spectrometer (ThermoFisher Scientific, Newington, NH, USA) was used for the ESI-MS (MS, mass spectrometry) studies. The spray source was customized using an outer stainless-steel capillary (0.5 mm i.d. and 1.6 mm o.d.) for the supply of nitrogen nebulizing gas and an inner fused silica capillary (100 μm i.d. and 360 μm o.d.) for the delivery of solvent/solution. The inner silica capillary tip was kept extended 1 mm outside the coaxial stainless-steel capillary orifice for better nebulization through the spray nozzle. Negatively charged microdroplets were generated in the negative-ion mode (−5 kV DC potential supplied to the stainless-steel needle of the solvent syringe) at a solvent flow rate of 5 μL/min via silica tubing with a coaxial sheath gas flow of high-purity nitrogen gas (≥99.9997%) at 110 psi backpressure. The spray voltage was also tuned from 0 to −5 kV as specified. The stream of charged microdroplets from the spray nozzle was focused on the heated (300 °C) mass spectrometer inlet capillary, which caused desolvation of the analyte ions. The distance from the spray tip to the mass spectrometer inlet was kept at 15 mm, and the maximum ion injection time was set to 500 ms with one microscan. The mass resolution was set to 120,000. The S-lens RF level was set to 69.5%. In order to obtain the highest ion current, additional ion optics were autotuned. Thermo Fisher Scientific's XCalibur software was used for data acquisition, each with a 1 min scan. The charged species were identified based on high mass (m/z) accuracy (<5 ppm error) and isotopic distribution pattern registered in the average (over 1 min) mass spectrum. All results were evaluated from triplicate measurements, and intensity values are presented as the mean value, wherever applicable. Unless otherwise stated, all experiments were conducted using the same instrumental parameters mentioned above.

Offline Collection and Analysis of the Sprayed Benzoic Acid Solution

10 mM benzoic acid or its different derivative solutions in water were aerosolized using a spray source similar to what was used in the ESI-MS experiment. The spray source was fitted to a two-neck round-bottom flask, as shown in Figure 3a. An infusion pump maintained the aryl acid solution flow rate at 40 μL/min through the spray source, while nitrogen was used as a sheath gas at a back pressure of 80 psi. The spray was allowed to travel a distance of 8 cm before hitting the bottom of the flask. One condenser (with cold water circulation) was connected to the other neck of the flask to reduce the product loss. The inside bottom of the flask was given the earth potential using an aluminum foil tape. After spraying for 2 h, the reaction mixture collected at the bottom of the flask was dissolved in 2 mL of methanol and submitted for gas chromatography (GC)-MS analysis.

Dual Channel Infusion Experiment for Monitoring the Aromatic Electrophilic *ipso*-Substitution in Microdroplets

Two 500 μL Hamilton syringes, one containing an aqueous solution of benzoic acid (100 μM) and the other having an aqueous solution of the electrophile (200 μM), were pumped each at a 3 μL/min flow rate through the narrow borosilicate capillary (100 μm i.d. and 360 μm o.d.) to a mixing tee. The mixed solution was afterward directed toward an electrospray source that operated at 110 psi nitrogen back pressure and a −5 kV voltage (applied to the benzoic acid-containing syringe needle). The distance between the spraying nozzle and the mass spectrometer inlet was kept constant at 15 mm. The aromatic electrophilic *ipso*-substitution product formed in microdroplets was determined from the corresponding ion signal in the MS1 spectrum and the MS/MS data of the mass-selected ion. The other MS instrumental parameters were similar to those of the aforementioned ESI-MS study.

GC-MS

The GC-MS analysis was performed using a gas chromatograph (Agilent Technologies, Model 7890B) coupled with an ion trap mass spectrometer (Agilent Technologies, Model 5977B). An Agilent J&W GC capillary column (30 m length, 0.25 mm i.d., 0.25 μm film thickness) was utilized in this study. Helium was used as the carrier gas (99.99% purity) and maintained at a constant flow rate of 1.6 mL/min. The GC column temperature program was as follows: initial temperature of 55 °C for 2 min, then 55−300 °C at 10 °C/min temperature ramp, and finally kept at 300 °C for 2 min. The methanolic solution (10 μL) of the analyte was injected in a split mode (50:1), and the temperature at the injector was kept at 280 °C. The MS conditions were as follows: electron ionization mode at an ionization energy of 70 eV and emission current of 250 μA; the ion source and transfer line temperatures were maintained at 250 and 280 °C, respectively. Standard samples were used to identify the retention times, and the products were further verified by matching the ion fragmentation pattern with a database in the software provided with the instrument.

RESULTS AND DISCUSSION

Figure 1 illustrates our experimental setup involving a custom-built ESI source coupled to a high-resolution (orbitrap) mass spectrometer. The spray source was operated at a −5 kV potential (also at 0 V as specified) with a 5 μL/min solution flow and 110 psi back pressure of nitrogen as the nebulizing gas. Three different aqueous aromatic acid solutions (benzoic acid, phenylsulfinic acid, and phenylboronic acid), each with 100 μM concentration, were sprayed toward the mass spectrometer to analyze the chemical contents of the aerosolized microdroplets (average size of 4 μm[1]). We detected phenyl carbanion (Ph^-) spontaneously formed from precursor aryl acids in the water microdroplets (Figure 1b). This reactive species (Ph^-) was characterized by its mass-to-charge ratio (m/z) with high accuracy (Table S1). This transformation efficiency followed the order Ph−COOH > Ph-SO_2H > Ph-$B(OH)_2$ in generating Ph^- in water microdroplets (Figure S1). This result also corroborates our observation that benzoic and phenylsulfinic acids readily produced Ph^- under 0 V spray, whereas no such detection was made for phenylboronic acid (Figure S2). The lower performance of Ph-$B(OH)_2$ in producing Ph^- in microdroplets, compared to the other aromatic acids, can be attributed to its weak acidity (pK_a ∼ 8.8), limiting its dissociation in aqueous medium, resulting in insufficient formation of phenylboronate (the conjugate base), which is likely the actual precursor to Ph^-. We also conducted molecular dynamics (MD) simulations which revealed a relatively lower surface enrichment of phenylsulfinic acid compared to that of benzoic acid in aqueous microdroplets (Figure S3). This computational result aligns with our experimental observation, which shows a higher yield of Ph^- from $PhCO_2H$ than Ph-SO_2H, likely occurring at or near the surface of the microdroplets (vide infra). On increasing the pH of the aqueous solution of benzoic acid, the Ph^- ion intensity increased, indicating the role of OH^- on the acid

https://doi.org/10.1021/jacsau.4c00810
JACS Au 2024, 4, 4488−4495

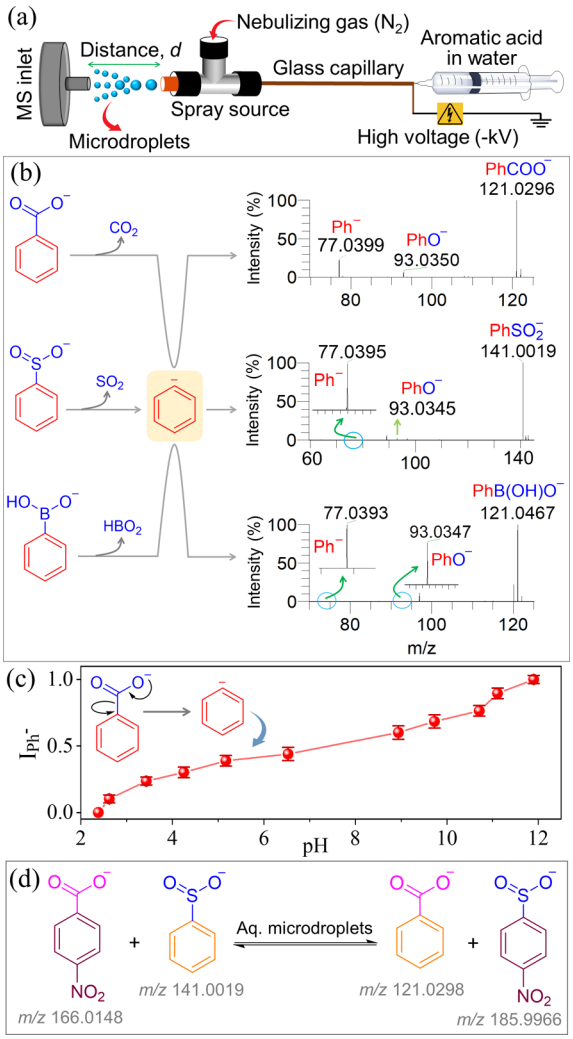

Figure 1. (a) Experimental setup for spraying aqueous solution of aromatic acids to a mass spectrometer. (b) Negative-ion mode ESI-MS investigation of the microdroplet reaction of three different aromatic acids sprayed from the respective aqueous solution revealed the spontaneous formation of phenyl carbanion (Ph^-) and phenoxide anion. (c) MS monitoring of the generation of Ph^- in the sprayed aerosol on varying the pH of the aqueous benzoic acid solution. The pH was maintained by adding HCOOH or NaOH to the solution. The Ph^- intensity data are normalized to 1 in the plot, and error bars correspond to standard deviation from triplicate measurements. (d) MS monitoring of the functional group exchange reaction between *p*-nitrobenzoic acid and phenylsulfinic acid in aqueous microdroplets.

deprotonation followed by decarboxylation reaction in microdroplets (Figures 1c and S4). As the in-droplet OH^- formation is facilitated by water reduction under −5 kV spray,[43,44] Ph^- detection (Figure 1b) was also accompanied by the reaction of leaving groups with OH^-, resulting in the formation of HCO_3^- from Ph−COOH, HSO_3^- from Ph-SO_2H, and $H_2BO_3^-$ from Ph-B(OH)$_2$ in microdroplets (Figure S5). We also noted that water or water-containing microdroplets outperformed organic microdroplets in producing and stabilizing Ph^- (Figure S6), possibly due to the prevalence of OH^- and subsequent high negative charge density in the electrosprayed water droplets.[44] When a mixture of two different aryl acids in water was sprayed, we observed a functional group exchange reaction (Figures 1d and S7), indicating the reversibility of Ph^- formation from the deprotonated precursor aryl acid.

We extended our study to include different benzoic acid derivatives with electron-withdrawing and -donating substituents (Table S2). In all cases, decarboxylative generation of aryl carbanions in microdroplets was observed under both −5 kV (Figure 2) and 0 V (Figure S8) spray conditions. These observations highlight that a high voltage is not necessarily required to generate and stabilize aryl carbanions in water microdroplets. A significant fraction of the droplets produced without applying any potential can still hold negative charges due to the statistical fluctuation of ions (H^+/OH^-)[45−48] or the liquid−gas contact electrification process.[25] However, application of a negative spray potential enhances the production and stability of aryl carbanion due to high negative charge density (e.g., OH^- obtained from the reduction of water at the electrospray emitter) in the sprayed microdroplets (vide infra).[36,43,49] Generally, the lifetime of reactive carbanion ranges from nanoseconds to picoseconds in the bulk medium.[36] The survival of highly reactive aryl carbanions in microdroplets with a typical lifetime of around a millisecond[49] suggests their enhanced stability by over a million times compared to the bulk phase.

It should also be noted that the relative intensity of the aryl carbanion compared to that of its precursor aryl carboxylate in the mass spectra (Figure 2) is not directly correlated with the electronic effects of substituents in the precursor. This may hint that the decarboxylation occurs at the surface of the microdroplet, where the molecular orientation is crucial for experiencing interfacial effects (such as surface pH, partial solvation, and intrinsic electric fields) in addition to the electronic effects of substituents. Substituents in aryl acid substrates likely cause differential experiences of these interfacial effects. Interestingly, the steric hindrance in 2,4,6-trimethylbenzoate appears to facilitate the decarboxylation, forming the corresponding aryl carbanion species (Figure 2i). Once formed, this species is less likely to be annihilated (by reacting with an electrophile) in water microdroplets due to steric hindrance imparted by methyl groups, giving rise to an intense peak of the aryl carbanion in the mass spectrum. Conversely, the relative intensity of the aryl carbanion peak obtained from spraying 2,4-dimethoxybenzoic acid is lower, likely because the dominant electron-donating effect of the methoxy groups outweighs the steric effect, thus, somewhat destabilizing the aryl carbanion (Figure 2f).

We investigated the formation of three typical aryl carbanions from aryl carboxylic and phenylsulfinic acids in water microdroplets by varying the spray parameters, such as the nebulizing gas pressure, the solution flow rate, the spray tip-to-MS inlet distance, and the spray voltage (Figures S9−S12). When these parameters resulted in smaller-sized microdroplets with a higher surface-to-volume ratio (Supplementary Note 1), the abundance of the carbanion increased, suggesting that the conversion of those aryl acids to Ph^- preferentially occurs at the microdroplet surface. The crucial role of the surface (air−water interface) in promoting this reaction is discussed later. Moreover, the abundance of Ph^- positively correlated with the concentration of benzoic acid in microdroplets (Figure S13), possibly indicating the first-order kinetics of the decarboxylation process (generation of Ph^-). It should also be noted that the dependence of the reaction on the surface-to-volume ratio of the microdroplet, its preference for water over organic microdroplets (Figure S6), and the observation of functional group exchange (Figure 1d) can be

https://doi.org/10.1021/jacsau.4c00810
JACS Au 2024, 4, 4488−4495

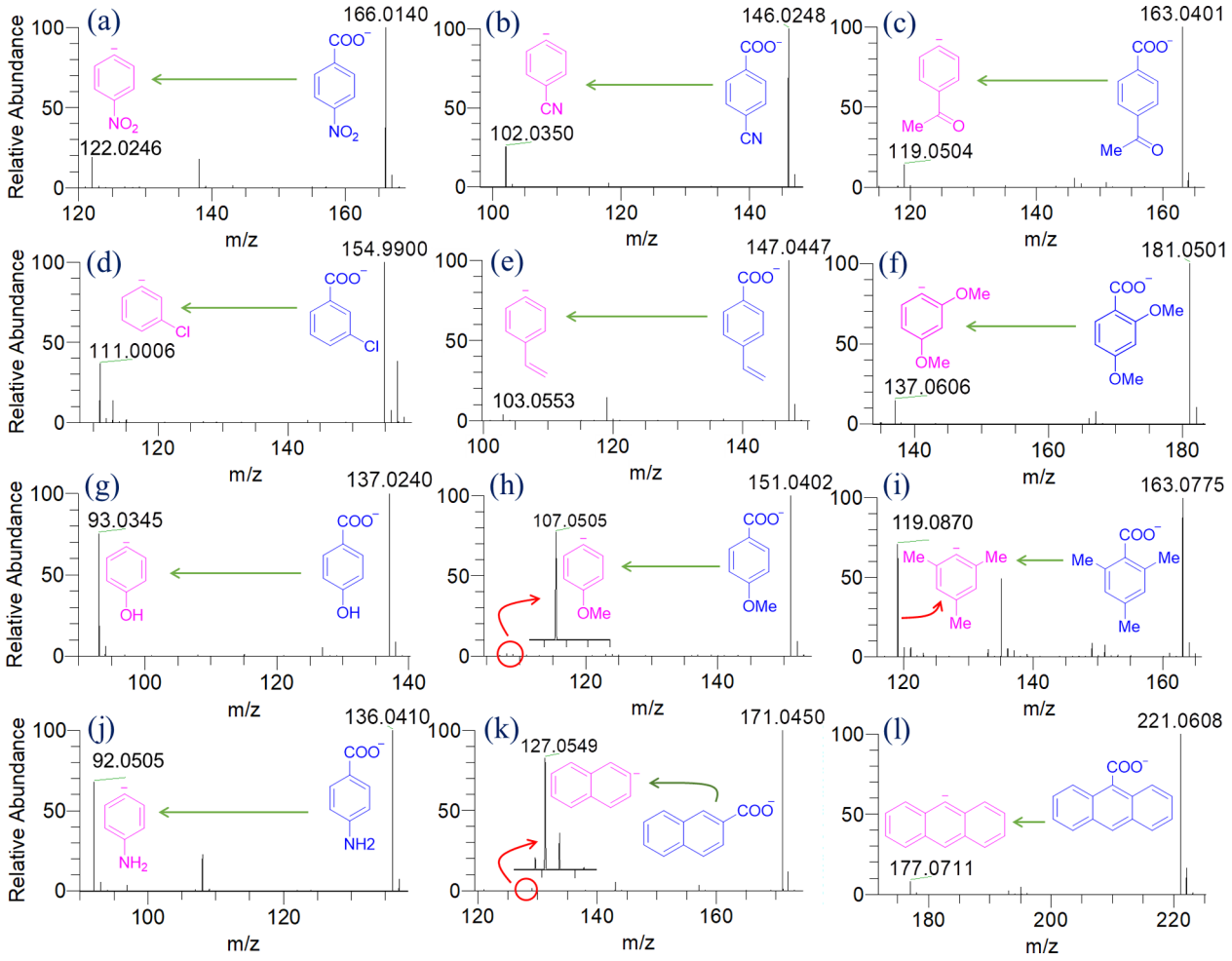

Figure 2. Negative-ion mode ESI-mass spectra (a–l) revealed that aryl carboxylic acids spontaneously produce aryl carbanions (shown in insets) in water microdroplets by the Csp^2–COOH bond cleavage (decarboxylation process). Analogous mass spectra obtained from 0 V spray are shown in Figure S8.

taken into account to rule out the unlikely possibility of the reaction occurring in the gas phase (outside the droplet).

We speculated that Ph^-, being a strong base, might react with H^+ in water microdroplets to yield benzene, which would remain undetected in ESI-MS. To ensure the formation of benzene by the protodecarboxylation process, we collected the sprayed microdroplets in a flask using an offline experimental setup (Figures 3a and S14) followed by analysis using GC-MS. Thus, we detected 11% conversion of benzoic acid to benzene in water microdroplets. This protodecarboxylation efficiency was increased by an electron-withdrawing group and decreased by an electron-donating group attached to the aromatic ring. For example, spraying of *p*-nitrobenzoic acid and *p*-aminobenzoic acid yielded 29% nitrobenzene and 8% aniline, respectively (Figure 3a). This result relates to the intermediate aryl carbanion stability influenced by the other functional groups in the protodecarboxylation process. Analogously, spraying a mixture of *p*-nitrobenzoic acid and methyl iodide yielded two products: 12% nitrobenzene and 16% *p*-nitrotoluene (Figure 3a). This result is attributed to the competitive reaction of two electrophiles (proton and methyl iodide) with the intermediate *p*-nitrophenyl carbanion produced in the aqueous microdroplets. All of the above quantifications of the offline reaction products were performed by GC–MS analyses based on standard chromatograms and calibration plots (Figures S15–S19).

An earlier study from the Zare group reported decarboxylative hydroxylation of benzoic acid to yield ~5% phenol in water microdroplets.[49] Under the analogous spray conditions, while we also traced the phenol formation (*m*/*z* 93.0345 in Figure 1b), we decipher here protodecarboxylation of benzoic acid as another dominant reaction pathway occurring concurrently in water microdroplets (Figure 3b). As we found no evidence of the formation of benzoate radical species in water microdroplets (Figure S20a), we propose that the benzoate anion is the precursor of Ph^- (Figure 1c). This Ph^- either can react with the droplet proton (electrophile) to yield benzene or can liberate an electron to generate a phenyl radical (Figures S20 and S21), which may then combine with a hydroxyl radical to produce phenol at the air–water interface (Figure 3b). The localized high electric field at the microdroplet surface might facilitate the ejection of an electron (oxidation) from Ph^-, leading to the generation of a phenyl radical (Supplementary Note 2).[50−53] Although the phenyl radical is likely more stable than Ph^-, the relatively greater reactivity of the latter for electrophilic addition (a barrierless process) warrants its rapid protonation at the air–water interface (Supporting Information, Note 3). That Ph^- is a precursor of benzene was further confirmed by the observation

https://doi.org/10.1021/jacsau.4c00810
JACS Au 2024, 4, 4488–4495

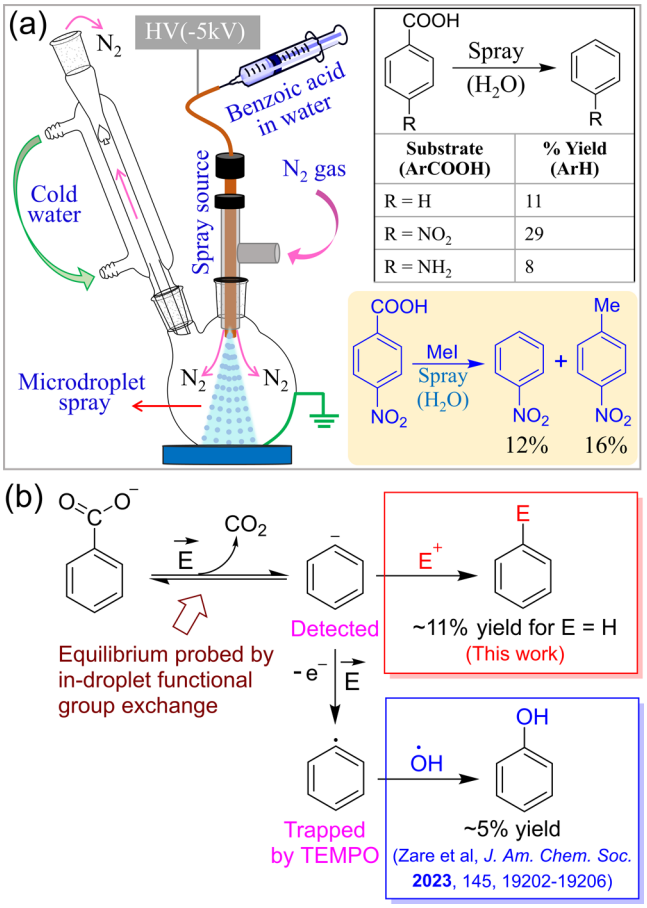

Figure 3. (a) Diagram of an offline experimental setup for spraying the aqueous solution of aryl carboxylic acids under −5 kV potential in a round-bottom flask followed by the analysis of the resulting reaction mixture by GC−MS for quantifying the corresponding decarboxylated yields (Figures S15−S19) as tabulated in the inset. (b) A plausible mechanism of the benzoic acid decarboxylation, generating highly reactive Ph^-, which can either combine with an electrophile (major pathway) or transform into a phenyl radical, followed by the capture of hydroxyl radical to yield phenol (minor pathway) at the air−water interface of microdroplets in less than a millisecond.

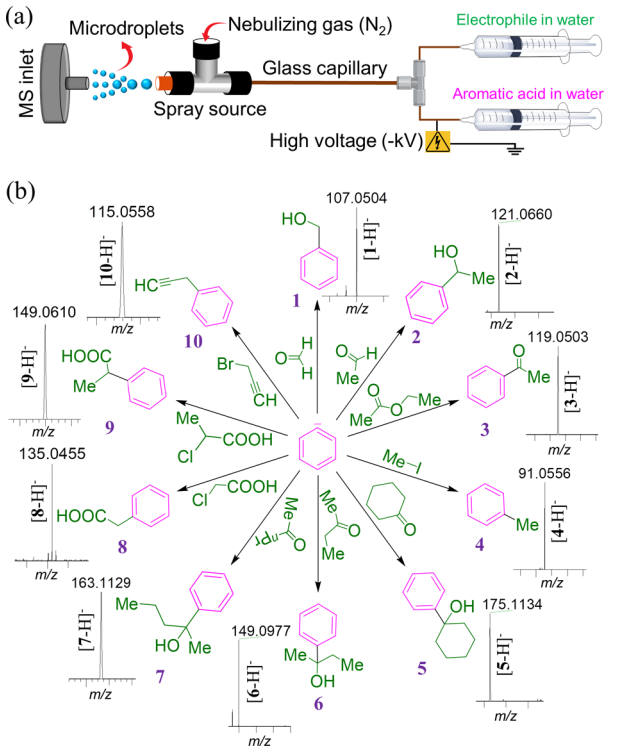

Figure 4. (a) Experimental setup for infusing benzoic acid and electrophile solutions into a spray source for performing electrophilic *ipso*-substitution at the air−water interface of microdroplets. (b) Ph^- generated in water microdroplets was allowed to react with different electrophiles, yielding *ipso*-substitution products of benzoic acid (**1**−**10**). These products (deprotonated) were detected by MS, and the ion signal of each species is presented next to its respective structure. For convenience in the presentation, only the target product peaks are shown, some of which were characterized using MS/MS (Figures S22−S26).

of the electrophilic *ipso*-substitution of benzoic acid in water microdroplets (see below). However, we do not rule out the possibility of the partial involvement of another route for in-droplet benzene formation through the reaction of a phenyl radical with a hydrogen radical, considering that water microdroplets may also generate hydrogen radicals in addition to hydroxyl radicals.[10,24,54]

As Ph^- is spontaneously generated from benzoic acid at the air−water interface, we performed a series of electrophilic *ipso*-substitution of benzoic acid in water microdroplets by infusing aqueous benzoic acid and electrophile solutions into the spray source using a dual-channel infusion pump (Figure 4a). A −5 kV spray potential generated negatively charged microdroplets with a high electric field at the air−water interface. MS was employed to analyze the chemical contents of these microdroplets. Thus, we observed that the Ph^- generated in microdroplets could react with various electrophiles (e.g., carbonyls, esters, methyl iodide, α-halo carboxylic acids, and 3-bromopropyne), yielding the *ipso*-substitution products of benzoic acid **1**−**10** (Figure 4b). The product species were identified by high mass accuracy (Table S3) and MS/MS (Figures S22−S26). We attempted to quantify one representative product **8**, which gave rise to an intense peak at *m*/*z* 135.0455 (Figure 4b). Given that the ionization efficiency of Ph−COOH is at least 10 times higher than that of Ph−CH_2COOH (Figure S27), the in-droplet transformation of the former to the latter reached up to 26% at a spray distance of 5 cm (Figure S28). Considering this result and the simultaneous formation of benzene (Figure 3b), we infer >30% conversion of benzoic acid to Ph^- in the sprayed microdroplets. Analogously, Ph^- obtained from phenylsulfinic acid in water microdroplets was reacted with different electrophiles to yield the corresponding *ipso*-substitution products (Figure S29). It is important to clarify that we performed the above reactions (Figure 4) by separately infusing the substrate and the electrophile into a tee-junction, followed by immediate electrospraying to the mass spectrometer inlet to ensure that any bulk reaction before the sample infusion does not interfere with the reactions in microdroplets. Moreover, as previously explained, the role of nitrogen in the spray source is exclusively for atomizing the solution, which affects the droplet size and speed and, thereby, the reaction yield. We do not have any evidence that this nitrogen participates in the reaction mechanism. Indeed, we observed that the reaction also occurs in microdroplets generated from a paper spray ionization source, where no nitrogen nebulizing gas is used (Figure S30).

An MD simulation deciphered that benzoate in microdroplets is surface active and prefers to reside at the air−water

https://doi.org/10.1021/jacsau.4c00810
JACS Au 2024, 4, 4488−4495

interface (Figures 5a and S31a) with the aromatic ring oriented toward the air side and the carboxylate group immersed in water (Figures S31b and S32). Such an orientation possibly allows the benzoic acid to experience a high electric field at the surface, which can weaken the benzoate C−COO$^-$ bond. Indeed, DFT calculations indicated that a high electric field (~10^8 V/cm) could weaken and facilitate the heterolytic cleavage of the benzoate C−COO$^-$ bond (Figure 5b), resulting in Ph$^-$ (Figure 5c). These results align with our experimental finding that the reaction is facilitated by the high surface-to-volume ratio (Figure S8a−c) and the increase of negative charge density (and thus the electric field at the interface; Figure S9d) of microdroplets. The heterolytic nature of the bond cleavage is further reinforced by the observation that higher pH levels in the droplet solvent result in a better formation of Ph$^-$ (Figures 1c and S4). Moreover, there is no experimental evidence on the generation of aryl carboxyl radical in microdroplets (Figure S20a) to propose that the above bond cleavage is homolytic through an alternate mechanism. Therefore, we believe that the decarboxylation process of benzoic acid at the air−water interface is heterolytic, as shown in Figure 3b, and the resulting Ph$^-$ (detected) is readily captured by an electrophile (Figures 3b and 4b) present in the microdroplet as a major route of its annihilation.

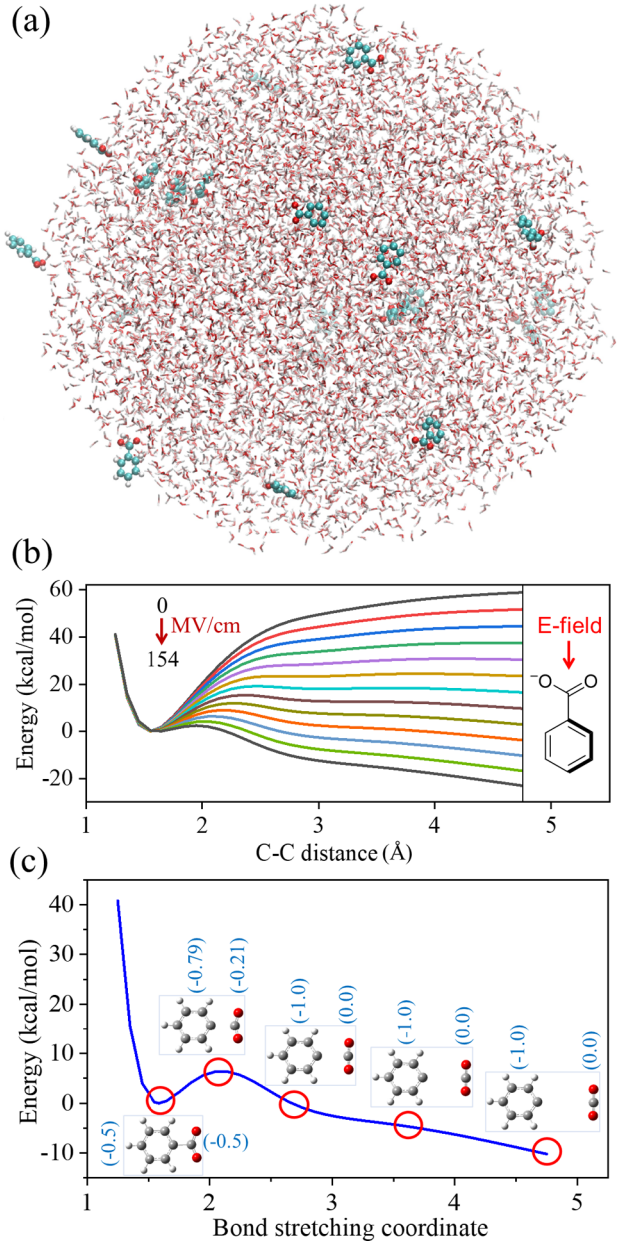

Figure 5. (a) Average snapshot obtained from MD simulation for a water nanodroplet containing benzoic acid (7028 water molecules and 20 benzoic acid molecules), showing the preferential distribution of benzoic acid at the droplet surface (Figure S31). (b) Electronic structure calculations using the M062X/cc-pVTZ level of theory. Potential energy profile along Ph−COO$^-$ bond stretching of benzoate anion under varying external electric fields along the Ph−COO$^-$ bond direction, as shown in the inset. (c) Potential energy profile for the decarboxylation of benzoate anion under a 128.5 MV/cm electric field in the gas phase, showing the gradual change of the structure and associated charges of the species in the insets.

CONCLUSIONS

In summary, we reveal that three different aryl acids (benzoic, phenylsulfinic, and phenylboronic acids) spontaneously undergo heterolytic fission of Csp^2−C, Csp^2−S, or Csp^2−B bonds, generating aryl carbanions at the air−water interface of the microdroplets. An intrinsic ultrahigh electric field on the microdroplet surface weakens those bonds, which is further facilitated by the appropriate molecular orientation of the partially desolvated substrate at the interface. The aryl carbanions thus formed are stabilized at the water-deficient interface before reacting with an electrophile (proton or an organic compound), producing the *ipso*-substitution product.

ASSOCIATED CONTENT

Supporting Information

The Supporting Information is available free of charge at https://pubs.acs.org/doi/10.1021/jacsau.4c00810.

Materials and methods, computational methods, bar plot, ESI-MS spectra, MD simulation, GC-MS chromatogram, mass spectral data, and DFT details (PDF)

AUTHOR INFORMATION

Corresponding Author

Shibdas Banerjee − *Department of Chemistry, Indian Institute of Science Education and Research Tirupati, Tirupati 517507, India;* orcid.org/0000-0002-3424-8157; Email: shibdas@iisertirupati.ac.in

Authors

Abhijit Nandy − *Department of Chemistry, Indian Institute of Science Education and Research Tirupati, Tirupati 517507, India*

Hariharan T − *Department of Chemistry, Indian Institute of Science Education and Research Tirupati, Tirupati 517507, India*

Deepsikha Kalita − *Department of Chemistry, Indian Institute of Technology Hyderabad, Kandi 502284, India*

Debasish Koner − *Department of Chemistry, Indian Institute of Technology Hyderabad, Kandi 502284, India;* orcid.org/0000-0002-5116-4908

Complete contact information is available at: https://pubs.acs.org/10.1021/jacsau.4c00810

https://doi.org/10.1021/jacsau.4c00810
JACS Au 2024, 4, 4488−4495

Author Contributions

S.B. designed and supervised the research; A.N. and H.T. performed the experiments; A.N. and S.B. analyzed the data; D.K. and D.K. performed theoretical studies; S.B., A.N., and D.K. wrote the paper. CRediT: **Shibdas Banerjee** conceptualization, funding acquisition, resources, supervision.

Notes

The authors declare no competing financial interest.

■ ACKNOWLEDGMENTS

The authors thank the SERB and DST, India, for supporting this work (grant numbers CRG/2022/002676 and DST/INSPIRE/04/2019/002108). D.K. acknowledges the support from the IIT Hyderabad Seed Grant (No. SG/IITH/F328/2023-24/SG-164).

■ REFERENCES

(1) Nandy, A.; Kumar, A.; Mondal, S.; Koner, D.; Banerjee, S. Spontaneous Generation of Aryl Carbocations from Phenols in Aqueous Microdroplets: Aromatic SN1 Reactions at the Air−Water Interface. *J. Am. Chem. Soc.* **2023**, *145* (29), 15674−15679.
(2) Meng, Y.; Gnanamani, E.; Zare, R. N. Direct C(sp3)−N Bond Formation between Toluene and Amine in Water Microdroplets. *J. Am. Chem. Soc.* **2022**, *144* (43), 19709−19713.
(3) Meng, Y.; Zare, R. N.; Gnanamani, E. One-Step, Catalyst-Free Formation of Phenol from Benzoic Acid Using Water Microdroplets. *J. Am. Chem. Soc.* **2023**, *145* (35), 19202−19206.
(4) Song, X.; Basheer, C.; Xia, Y.; Li, J.; Abdulazeez, I.; Al-Saadi, A. A.; Mofidfar, M.; Suliman, M. A.; Zare, R. N. One-step Formation of Urea from Carbon Dioxide and Nitrogen Using Water Microdroplets. *J. Am. Chem. Soc.* **2023**, *145* (47), 25910−25916.
(5) Song, X.; Basheer, C.; Zare, R. N. Making ammonia from nitrogen and water microdroplets. *Proc. Natl. Acad. Sci., U. S. A.* **2023**, *120* (16), No. e2301206120.
(6) Zhang, D.; Yuan, X.; Gong, C.; Zhang, X. High Electric Field on Water Microdroplets Catalyzes Spontaneous and Ultrafast Oxidative C−H/N−H Cross-Coupling. *J. Am. Chem. Soc.* **2022**, *144* (35), 16184−16190.
(7) Meng, Y.; Gnanamani, E.; Zare, R. N. One-Step Formation of Pharmaceuticals Having a Phenylacetic Acid Core Using Water Microdroplets. *J. Am. Chem. Soc.* **2023**, *145* (14), 7724−7728.
(8) Song, X.; Meng, Y.; Zare, R. N. Spraying Water Microdroplets Containing 1,2,3-Triazole Converts Carbon Dioxide into Formic Acid. *J. Am. Chem. Soc.* **2022**, *144* (37), 16744−16748.
(9) Chen, H.; Wang, R.; Xu, J.; Yuan, X.; Zhang, D.; Zhu, Z.; Marshall, M.; Bowen, K.; Zhang, X. Spontaneous Reduction by One Electron on Water Microdroplets Facilitates Direct Carboxylation with CO2. *J. Am. Chem. Soc.* **2023**, *145* (4), 2647−2652.
(10) Song, X.; Basheer, C.; Zare, R. N. Water Microdroplets-Initiated Methane Oxidation. *J. Am. Chem. Soc.* **2023**, *145* (50), 27198−27204.
(11) Zhang, W.; Yang, S.; Lin, Q.; Cheng, H.; Liu, J. Microdroplets as Microreactors for Fast Synthesis of Ketoximes and Amides. *J. Org. Chem.* **2019**, *84* (2), 851−859.
(12) Zheng, B.; Jin, X.; Liu, J.; Cheng, H. Accelerated Metal-Free Hydration of Alkynes within Milliseconds in Microdroplets. *ACS Sust. Chem. Eng.* **2021**, *9* (12), 4383−4390.
(13) Zhang, W.; Zheng, B.; Jin, X.; Cheng, H.; Liu, J. Rapid Epoxidation of α,β-Unsaturated Olefin in Microdroplets without Any Catalysts. *ACS Sust. Chem. Eng.* **2019**, *7* (17), 14389−14393.
(14) Xue, L.; Zheng, B.; Sun, J.; Liu, J.; Cheng, H. Water Microdroplet Chemistry for Accelerating Green Thiocyanation and Discovering Water-Controlled Divergence. *ACS Sust. Chem. Eng.* **2023**, *11* (34), 12780−12789.
(15) Girod, M.; Moyano, E.; Campbell, D. I.; Cooks, R. G. Accelerated bimolecular reactions in microdroplets studied by desorption electrospray ionization mass spectrometry. *Chem. Sci.* **2011**, *2* (3), 501−510.
(16) Nandy, A.; Mondal, S.; Koner, D.; Banerjee, S. Heavy Water Microdroplet Surface Enriches the Lighter Isotopologue Impurities. *J. Am. Chem. Soc.* **2024**, *146* (28), 19050−19058.
(17) Hao, H.; Leven, I.; Head-Gordon, T. Can electric fields drive chemistry for an aqueous microdroplet? *Nat. Commun.* **2022**, *13* (1), 280.
(18) Xiong, H.; Lee, J. K.; Zare, R. N.; Min, W. Strong Electric Field Observed at the Interface of Aqueous Microdroplets. *J. Phys. Chem. Lett.* **2020**, *11* (17), 7423−7428.
(19) Qiu, L.; Cooks, R. G. Simultaneous and Spontaneous Oxidation and Reduction in Microdroplets by the Water Radical Cation/Anion Pair. *Angew. Chem., Int. Ed.* **2022**, *61* (41), No. e202210765.
(20) Jin, S.; Chen, H.; Yuan, X.; Xing, D.; Wang, R.; Zhao, L.; Zhang, D.; Gong, C.; Zhu, C.; Gao, X.; Chen, Y.; Zhang, X. The Spontaneous Electron-Mediated Redox Processes on Sprayed Water Microdroplets. *J. Am. Chem. Soc. Au* **2023**, *3* (6), 1563−1571.
(21) Mofidfar, M.; Mehrgardi, M. A.; Xia, Y.; Zare, R. N. Dependence on relative humidity in the formation of reactive oxygen species in water droplets. *Proc. Natl. Acad. Sci., U. S. A.* **2024**, *121* (12), No. e2315940121.
(22) Lee, J. K.; Walker, K. L.; Han, H. S.; Kang, J.; Prinz, F. B.; Waymouth, R. M.; Nam, H. G.; Zare, R. N. Spontaneous generation of hydrogen peroxide from aqueous microdroplets. *Proc. Natl. Acad. Sci., USA* **2019**, *116* (39), 19294−19298.
(23) Heindel, J. P.; LaCour, R. A.; Head-Gordon, T. The role of charge in microdroplet redox chemistry. *Nat. Commun.* **2024**, *15* (1), 3670.
(24) Colussi, A. J. Mechanism of Hydrogen Peroxide Formation on Sprayed Water Microdroplets. *J. Am. Chem. Soc.* **2023**, *145* (30), 16315−16317.
(25) Kumar, A.; Avadhani, V. S.; Nandy, A.; Mondal, S.; Pathak, B.; Pavuluri, V. K. N.; Avulapati, M. M.; Banerjee, S. Water Microdroplets in Air: A Hitherto Unnoticed Natural Source of Nitrogen Oxides. *Anal. Chem.* **2024**, *96* (26), 10515−10523.
(26) Nam, I.; Lee, J. K.; Nam, H. G.; Zare, R. N. Abiotic production of sugar phosphates and uridine ribonucleoside in aqueous microdroplets. *Proc. Natl. Acad. Sci., USA* **2017**, *114* (47), 12396−12400.
(27) Holden, D. T.; Morato, N. M.; Cooks, R. G. Aqueous microdroplets enable abiotic synthesis and chain extension of unique peptide isomers from free amino acids. *Proc. Natl. Acad. Sci., U. S. A.* **2022**, *119* (42), No. e2212642119.
(28) Wang, W.; Qiao, L.; He, J.; Ju, Y.; Yu, K.; Kan, G.; Guo, C.; Zhang, H.; Jiang, J. Water Microdroplets Allow Spontaneously Abiotic Production of Peptides. *J. Phys. Chem. Lett.* **2021**, *12* (24), 5774−5780.
(29) Ju, Y.; Zhang, H.; Wang, X.; Liu, Y.; Yang, Y.; Kan, G.; Yu, K.; Jiang, J. Abiotic synthesis with plausible emergence for primitive phospholipid in aqueous microdroplets. *J. Colloid Interface Sci.* **2023**, *634*, 535−542.
(30) Vaida, V.; Deal, A. M. Peptide synthesis in aqueous microdroplets. *Proc. Natl. Acad. Sci., U. S. A.* **2022**, *119* (44), No. e2216015119.
(31) Enami, S.; Stewart, L. A.; Hoffmann, M. R.; Colussi, A. J. Superacid Chemistry on Mildly Acidic Water. *J. Phys. Chem. Lett.* **2010**, *1* (24), 3488−3493.
(32) Colussi, A. J.; Enami, S.; Ishizuka, S. Hydronium Ion Acidity Above and Below the Interface of Aqueous Microdroplets. *ACS Earth Space Chem.* **2021**, *5* (9), 2341−2346.
(33) Enami, S.; Colussi, A. J. Criegee Chemistry on Aqueous Organic Surfaces. *J. Phys. Chem. Lett.* **2017**, *8* (7), 1615−1623.
(34) Kumar, A.; Mondal, S.; Banerjee, S. Aqueous Microdroplets Capture Elusive Carbocations. *J. Am. Chem. Soc.* **2021**, *143* (6), 2459−2463.
(35) Kumar, A.; Mondal, S.; Sandeep; Venugopalan, P.; Kumar, A.; Banerjee, S. Destabilized Carbocations Caged in Water Microdroplets: Isolation and Real-Time Detection of α-Carbonyl Cation Intermediates. *J. Am. Chem. Soc.* **2022**, *144* (8), 3347−3352.

https://doi.org/10.1021/jacsau.4c00810
JACS Au 2024, 4, 4488−4495

(36) Kumar, A.; Mondal, S.; Mofidfar, M.; Zare, R. N.; Banerjee, S. Capturing Reactive Carbanions by Microdroplets. *J. Am. Chem. Soc.* **2022**, *144* (17), 7573−7577.
(37) Kumar, A.; Mondal, S.; Banerjee, S. Efficient Desorption and Capture of Reactive Carbocations from Positively Charged Glass Surface Bombarded with High-Speed Water Microdroplets. *J. Phys. Chem. C* **2023**, *127* (14), 6662−6669.
(38) Banerjee, S. On the stability of carbocation in water microdroplets. *Int. J. Mass Spectrom.* **2023**, *486*, No. 117024.
(39) Goossen, L. J.; Rodríguez, N.; Linder, C. Decarboxylative Biaryl Synthesis from Aromatic Carboxylates and Aryl Triflates. *J. Am. Chem. Soc.* **2008**, *130* (46), 15248−15249.
(40) Lai, R.-Y.; Chen, C.-L.; Liu, S.-T. In Situ Generated Palladium Nanoparticles for Catalytic Dehalogenation of Aryl Halides and Deboronation of Arylboronic acids. *J. Chin. Chem. Soc.* **2006**, *53* (4), 979−985.
(41) Chu, X.-Q.; Ge, D.; Cui, Y.-Y.; Shen, Z.-L.; Li, C.-J. Desulfonylation via Radical Process: Recent Developments in Organic Synthesis. *Chem. Rev.* **2021**, *121* (20), 12548−12680.
(42) Seo, S.; Taylor, J. B.; Greaney, M. F. Protodecarboxylation of benzoic acids under radical conditions. *Chem. Commun.* **2012**, *48* (66), 8270−8272.
(43) Banerjee, S.; Mazumdar, S. Electrospray Ionization Mass Spectrometry: A Technique to Access the Information beyond the Molecular Weight of the Analyte. *Int. J. Anal. Chem.* **2012**, *2012*, No. 282574.
(44) Blades, A. T.; Ikonomou, M. G.; Kebarle, P. Mechanism of electrospray mass spectrometry. Electrospray as an electrolysis cell. *Anal. Chem.* **1991**, *63* (19), 2109−2114.
(45) Xia, Y.; Xu, J.; Li, J.; Chen, B.; Dai, Y.; Zare, R. N. Visualization of the Charging of Water Droplets Sprayed into Air. *J. Phys. Chem. A* **2024**, *128* (28), 5684−5690.
(46) Zilch, L. W.; Maze, J. T.; Smith, J. W.; Ewing, G. E.; Jarrold, M. F. Charge Separation in the Aerodynamic Breakup of Micrometer-Sized Water Droplets. *J. Phys. Chem. A* **2008**, *112* (51), 13352−13363.
(47) Dodd, E. E. The Statistics of Liquid Spray and Dust Electrification by the Hopper and Laby Method. *J. Appl. Phys.* **1953**, *24* (1), 73−80.
(48) Lin, S.; Cao, L. N. Y.; Tang, Z.; Wang, Z. L. Size-dependent charge transfer between water microdroplets. *Proc. Natl. Acad. Sci., U. S. A.* **2023**, *120* (31), No. e2307977120.
(49) Kebarle, P.; Verkerk, U. H. Electrospray: from ions in solution to ions in the gas phase, what we know now. *Mass Spectrom. Rev.* **2009**, *28* (6), 898−917.
(50) Lee, J. K.; Samanta, D.; Nam, H. G.; Zare, R. N. Micrometer-Sized Water Droplets Induce Spontaneous Reduction. *J. Am. Chem. Soc.* **2019**, *141* (27), 10585−10589.
(51) Xing, D.; Yuan, X.; Liang, C.; Jin, T.; Zhang, S.; Zhang, X. Spontaneous oxidation of I− in water microdroplets and its atmospheric implications. *Chem. Commun.* **2022**, *58* (89), 12447−12450.
(52) Li, K.; Guo, Y.; Nizkorodov, S. A.; Rudich, Y.; Angelaki, M.; Wang, X.; An, T.; Perrier, S.; George, C. Spontaneous dark formation of OH radicals at the interface of aqueous atmospheric droplets. *Proc. Natl. Acad. Sci., U. S. A.* **2023**, *120* (15), No. e2220228120.
(53) Heindel, J. P.; Hao, H.; LaCour, R. A.; Head-Gordon, T. Spontaneous Formation of Hydrogen Peroxide in Water Microdroplets. *J. Phys. Chem. Lett.* **2022**, *13* (43), 10035−10041.
(54) Chen, X.; Xia, Y.; Wu, Y.; Xu, Y.; Jia, X.; Zare, R. N.; Wang, F. Sprayed Oil−Water Microdroplets as a Hydrogen Source. *J. Am. Chem. Soc.* **2024**, *146* (15), 10868−10874.

https://doi.org/10.1021/jacsau.4c00810
JACS Au 2024, 4, 4488−4495